CORA Cork Open Research Archive
Cartlann Taighde Oscailte Chorcaí

Title	Multiple-view time-frequency distribution based on the empirical mode decomposition
Author(s)	Stevenson, Nathan J.; Mesbah, Mostefa; Boashash, Boualem
Publication date	2010-08
Original citation	Stevenson, NJ, Mesbah, M, Boashash, B; (2010) 'Multiple-view time-frequency distribution based on the empirical mode decomposition'. Iet Signal Processing, 4 (4) :447-456. doi: 10.1049/iet-spr.2009.0084
Type of publication	Article (peer-reviewed)
Link to publisher's version	http://dx.doi.org/10.1049/iet-spr.2009.0084 Access to the full text of the published version may require a subscription.
Rights	**© 2010 The Institution of Engineering and Technology. This paper is a postprint of a paper submitted to and accepted for publication in IET Signal Processing and is subject to Institution of Engineering and Technology Copyright. The copy of record is available at IET Digital Library.**
Item downloaded from	http://hdl.handle.net/10468/630

University College Cork, Ireland
Coláiste na hOllscoile Corcaigh

A multiple view time–frequency distribution based on the empirical mode decomposition

N.J. Stevenson, M. Mesbah, and B. Boashash

Abstract

This paper proposes a novel, composite time–frequency distribution (TFD) constructed using a multiple view approach. This composite TFD utilises the intrinsic mode functions (IMFs) of the empirical mode decomposition (EMD) to generate each view which are then combined using the arithmetic mean. This process has the potential to eliminate the inter-component interference generated by a quadratic TFD (QTFD), as the IMFs of the EMD are, in general, mono–component signals. The formulation of the multiple view TFD in the ambiguity domain results in faster computation, compared to a convolutive implementation in the time–frequency domain, and a more robust TFD in the presence of noise. The composite TFD, referred to as the EMD–TFD, was shown to generate a heuristically, more accurate representation of the distribution of time–frequency energy in a signal. It was also shown to have performance comparable to the WVD when estimating the instantaneous frequency (IF) of multiple signal components in the presence of noise.

Index Terms

nonstationary, time–frequency distributions, Wigner–Ville distribution, adaptive, ambiguity do-

N.J. Stevenson (corresponding author) is with the Neonatal Brain Research Group, College of Medicine and Health, University College Cork, Cork, Ireland, e-mail: n.stevenson@ucc.ie

M. Mesbah is with the Centre for Clinical Research, University of Queensland, Royal Brisbane and Women's Hospital, Herston, QLD 4029

B. Boashash is with the College of Engineering, University of Sharjah, Sharjah, UAE

main, empirical mode decomposition, Hilbert–Huang transform, intrinsic mode function, instantaneous frequency estimation

A multiple view time–frequency distribution based on the empirical mode decomposition

I. INTRODUCTION

The analysis of signals in a joint time–frequency domain has been useful for radar and sonar signal processing [2]. The ambiguity domain which is a two–dimensional (2D) Fourier transform of the Wigner-Ville distribution (WVD) has long been used in sonar and radar processing for determining target range and velocity [2]. The instantaneous frequency of a detected signal component can assist in target classification and identification, for example parabolic patterns in the time–frequency domain such as those generated by quadratic frequency modulated (FM) signals are often seen in passive sonar due to multiple path interference from the sea floor [3, pp. 617]. Patterns, or specific arrangements of signal components, in time–frequency distributions (TFDs) have also been used to classify artificial and mammalian underwater acoustics [3], [4]. Advances in the representation of signal energy in a joint time–frequency domain will improve classification and estimation of the FM or amplitude modulation (AM) of signal components in sonar and radar applications.

A significant class of real nonstationary signals (signals whose frequency content varies over time) can be represented using the signal model,

$$s(t) = \sum_{k=1}^{M} a_k(t) \cos\left(\phi_k(t)\right) \tag{1}$$

where, $s_k(t) = a_k(t) \cos\left(\phi_k(t)\right)$ is a signal component or monocomponent, M is the number of components, $a_k(t)$ is the amplitude and $\phi_k(t)$ is the phase (which is the anti–derivative of the FM or instantaneous frequency (IF)) of the kth component, [5]. The use of (1) as a nonstationary signal model results in signal components that are not unique. In fact, there are an infinite number of choices for $a_k(t)$, $\phi_k(t)$ and M that can result in $s(t)$ where the nonstationarity can be embedded into the AM, FM or both. In order to overcome these infinite choices, we typically constrain the definition of

a signal component as a contiguous region of significant time–frequency energy. An approximation

to the definitions of significant is determined using Bedrosian's theorem [6].

The representation of signals, defined using (1), for the extraction of signal components is an important problem in signal processing. There are a number of methods for representing the distribution

of the time–frequency energy. These include atomic decomposition, the Hilbert–Huang transform

(HHT) and linear, quadratic and affine TFDs [3], [7]–[9]. No single method is ideal for representing

all signals modelled by (1) and the application of each method is, as a result, highly signal dependent.

This paper investigates the combination of the empirical mode decomposition (EMD), the algorithm

underlying the HHT and quadratic TFDs (QTFDs) in order to overcome deficiencies in each method.

The class of QTFDs is defined as,

$$\rho_z(t,f) = W_z(t,f) \underset{(t,f)}{**} \gamma(t,f) \tag{2}$$

where $W_z(t,f)$ is the WVD, $*$ is the convolution operation, and $\gamma(t,f)$ is a distribution specific

kernel or filter (typically some form of 2D low pass filter). The WVD is defined as,

$$W_z(t,f) = \int_{-\infty}^{\infty} z(t + \tfrac{\tau}{2})\bar{z}(t - \tfrac{\tau}{2})e^{-j2\pi f\tau} \, d\tau \tag{3}$$

where, $\bar{z}(t)$ denotes the complex conjugate of $z(t)$, $z(t)$ is the analytic associate of the signal under

analysis, that is, $z(t) = s(t) + j\mathcal{H}\{s(t)\}$ where $\mathcal{H}$ is the Hilbert transform, f is frequency, t is time

and τ is time lag.

The major problem with QTFDs is the interference generated between signal components due to the

quadratic nature of the transform. This interference means that a QTFD represents a signal modelled

by (1) as [10],

$$W_z(t,f) = \sum_{k=1}^{M} W_{z_k}(t,f) + \sum_{i=1,j=1,i\neq j}^{M} W_{z_i,z_j}(t,f) \tag{4}$$

where the first summation represents the signal components and the second summation of cross–

WVDs, $W_{z_i,z_j}(t,f)$ – see [3], represents the interference terms. There have been several attempts to

remove this interference via filtering the WVD [10], [11]. These techniques are based on 2D low pass

filtering as the interference terms in (4) tend to be highly oscillatory and are, therefore, represented

in the outer regions of the ambiguity domain. Recent techniques have used adaptive filters to better differentiate between interference and signal energy in the ambiguity domain. The concept of adaptive techniques for representing nonstationary signals appeals as the fundamental problem of resolving the AM and FM elements of a signal component means that nonadaptive techniques are unable to offer high performance for a wide range of nonstationary signals. In this paper, we use the EMD to decompose a signal into several sub-signals, denoted as intrinsic mode functions (IMFs) in the nomenclature of the EMD. An optimal ambiguity domain filter is then defined for each IMF and the resultant optimal filter set is used to construct a composite TFD using a multiple view approach.

The EMD decomposes a signal according to (1) by estimating the signal envelope, using a spline fitted to the local maxima and minima, then iteratively subtracting the mean of this envelope from the signal. A time–frequency representation (the HHT) can be formed using estimates of $a_k(t)$ and $\phi_k(t)$. These functions are estimated using the magnitude and phase of their analytic associates. The estimation of these functions using such a method is prone to error from approximating the infinite impulse response function of the Hilbert transform with finite filters and the enhancement of high frequency noise due to a differentiation process.

The multiple view approach uses a series of different choices for $\gamma(t, f)$, called views, that are designed to align with the IF law of particular signal components in the QTFD [12], [13]. The major problem with a multiple–view TFD is that the choice of the views is purely arbitrary unless *a priori* information is known. The use of the EMD offers the possibility of implementing a set of views that more accurately differentiate between regions of interference and signal energy in the ambiguity domain. This is because each IMF is, in general, a monocomponent signal and should, therefore, generate no interference in a QTFD.

This suggests that an obvious choice for a composite TFD based on the EMD is,

$$\text{TFD}(t, f) = \sum_{k=1}^{M} \text{WVD}\{\text{IMF}_k(t)\} \tag{5}$$

The problem with such an implementation is that the EMD does not always accurately decompose multicomponent nonstationary signals, in terms of (1) [14]. Signals that have high bandwidth/duration,

transients or significant noise result in a decomposition that can be approximated by the output of a bank of stationary low pass filters with dyadically increasing cutoff frequencies, [15]. In addition, the EMD is sensitive to the sampling frequency, and the end conditions of the cubic spline fits [14], [16]. As a result, the EMD can only accurately represent a signal defined with respect to (1) if the signal components are suitably constrained. The solution is to design a sequence of filters that adapt according to the localisation of IMF energy in the ambiguity domain. Constraints can be placed on these filters to ensure that a meaningful composite TFD is generated even when the EMD is not accurately decomposing a signal. The resultant composite TFD is a high resolution, low interference TFD suitable for use on a wide range of signals.

II. The EMD–TFD

A multiple view TFD can be generated by combining a number of smoothed or filtered WVDs. This composite, multiple view TFD is a combination of several TFDs generated by a series of filters or views,

$$\gamma(t,f) = \{\gamma_1(t,f), ..., \gamma_n(t,f)\},$$

using the operator $\mathcal{R}$ (e.g. a logical OR operation, the arithmetic or geometric mean). The original filter set used was a series of Gabor atoms with linear IF laws [12]. The composite TFD can, therefore, be defined as,

$$\text{TFD}(t,f) = \mathcal{R}\left[\gamma(t,f) \underset{(t,f)}{**} \text{WVD}(t,f)\right] \tag{6}$$

This can be readily interpreted (when $\mathcal{R}$ is a linear operator) in the ambiguity domain as,

$$\text{TFD}(t,f) = \mathcal{R}\left[\int_{-\infty}^{\infty}\int_{-\infty}^{\infty} \mathbf{G}(\nu,\tau)\, A_z(\nu,\tau)e^{j2\pi(\nu t - f\tau)}d\nu\, d\tau\right] \tag{7}$$

where $\mathbf{G}(\nu,\tau)$ is the 2D Fourier transform of $\gamma(t,f)$ and $A_z(\nu,\tau)$ is the 2D Fourier transform of $\text{WVD}(t,f)$.

The shape of the 2D filter set, $\gamma(t,f)$, and the type of operator will determine the performance of the composite TFD for various nonstationary signals.

The multiple view technique is shown diagrammatically in Fig. 1(a). In the case of the EMD–TFD the signal views are generated using the IMFs of the EMD, see Fig. 1(b). The multiple view, EMD–TFD adaptively generates a set of 2D filters functions, $\mathbf{G}(\nu, \tau)$, in the ambiguity domain localised around the significant ambiguity energy ($|A^{\mathrm{imf}}(\nu, \tau)|^2$) of each IMF.

The proposed multiple view EMD–TFD uses the arithmetic mean as the operator. This operator is chosen as it offers similar performance compared with other operators (see Table I) and permits a simplified implementation of the multiple view approach, see (10). The arithmetic mean is calculated using L views. These views are constructed from a sequence of L IMFs (L is generally limited to $\log_2(N)$ where N is the signal length, [15]). Only the IMFs, with high energy, that contribute to a user defined approximation of the original signal (typically 95%) are used to limit the computational burden of the EMD–TFD. The ambiguity domain filters/views are defined as,

$$G_i(\nu, \tau) = G_i^{th}(\nu, \tau) \underset{(\nu, \tau)}{**} h(\nu, \tau), \qquad i = [1, ..., L] \tag{8}$$

where $h(\nu, \tau)$ is a 2D filter,

$$G_i^{th}(\nu, \tau) = \begin{cases} 1 & \text{when } |A_i^{\mathrm{imf}}(\nu, \tau)| \geq t_h \max(|A_i^{\mathrm{imf}}(\nu, \tau)|) \\ \\ 0 & \text{elsewhere} \end{cases} \tag{9}$$

where $A_i^{\mathrm{imf}}(\nu, \tau)$ is the ambiguity domain representation of the ith IMF and t_h is a user defined threshold (a value ranging on $[0, 1]$) where a smaller value results in a view with a lower cutoff in the ambiguity domain and a TFD with higher suppression of interference but lower resolution). This value also reflects the accuracy of the EMD with respect to (1), the higher the value, the closer the IMFs of the EMD are to true monocomponent signals. The choice of the filter (in this case we refer to its representation in the time–frequency domain) is arbitrary but, as a rule of thumb, long duration sinusoids with slowly varying IF laws require long duration, narrowband filters, long duration sinusoids with rapidly varying IF laws require medium duration, medium bandwidth filters and impulse functions require short duration, high bandwidth filters.

The EMD–TFD is then defined as,

$$\rho_{\text{emd}}(t, f) = \int_{-\infty}^{\infty} \int_{-\infty}^{\infty} \frac{1}{L} \left\{ \sum_{i=1}^{L} G_i(\nu, \tau) \right\} A_z(\nu, \tau) e^{j2\pi(\nu t - f\tau)} d\nu \, d\tau \tag{10}$$

III. THE PERFORMANCE OF THE EMD–TFD

The ability of the EMD–TFD to represent the time–frequency energy of a signal, with minimal interference, was investigated using goodness of fit measurements that were designed to compare a TFD with the ideal time–frequency representation. The measures outlined in [17] are used to heuristically assess TFD performance. The ability of the EMD–TFD to estimate the IF of multiple signal components was also investigated. The performance of the EMD–TFD was compared to several nonadaptive QTFDs and the adaptive radial Gaussian kernel (RGK) TFD proposed in [11].

A. Time–frequency energy localisation

The ability of the EMD–TFD to localise time–frequency energy was tested using a synthetic three component signal. This signal consists of a linear FM (LFM) component with increasing frequency, a LFM component with decreasing frequency and a quadratic FM (QFM) component, all with constant amplitude. It is defined as,

$$s(t) = \sum_{i=1}^{3} s_i(t) \tag{11}$$

where,

$$s_1(t) = \sin\left(1024\pi(0.075t^2 + 0.05t)\right)$$

$$s_2(t) = \sin\left(1024\pi(-0.075t^2 + 0.2t)\right)$$

$$s_3(t) = \sin\left(1024\pi(-0.2t^3 + 0.3t^2 + 0.3t)\right)$$

t ranges on [0,1] and is sampled as 512Hz. The ideal time–frequency representation is,

$$\rho_d(t, f) = \sum_{i=1}^{3} a_i(t)^2 \delta(f - f_i(t)) \tag{12}$$

where the IFs of the components are,

$$f_1(t) = 76.8t + 25.6$$

$$f_2(t) = -76.8t + 120.4$$

$$f_3(t) = -307.2t^2 + 307.2t + 153.6$$

and $a_1(t) = a_2(t) = a_3(t) = 1$, (see Fig. 2).

The ambiguity domain filter set, $\mathbf{G}(\nu, \tau)$, for the EMD–TFD is shown in Fig. 3.

The EMD–TFD, WVD, spectrogram, HHT, RGK, Choi–Williams distribution and modified B–distribution, in addition to a TFD constructed according to (5) called the WVD-EMD were used in comparison. The TFDs of the test signal generated by each method are shown in Fig. 4.

The performance measures used to assess the goodness of fit between the TFD under trial and the desired TFD are the 2D linear correlation coefficient, R_{id}, and the correlation between the ideal time–frequency representation and a truncated version of the TFD at a selected threshold, R_t. A TFD with high values for both correlations can be considered as a high resolution, low interference TFD. The linear correlation coefficient indicates the level of interference in the TFD (the higher the interference, the lower the correlation) and is defined as,

$$R_{\mathrm{id}} = \frac{\int \int \rho(t,f) \rho_{\mathrm{id}}(t,f) dt df}{\left(\int \int \rho(t,f)^2 dt df \int \int \rho_{\mathrm{id}}(t,f)^2 dt df \right)^{0.5}} \tag{13}$$

where $\rho_{\mathrm{id}}(t,f)$ is the ideal TFD, $\rho(t,f)$ is the TFD under comparison and the integrals are defined on $[0, \infty]$.

The second correlation coefficient indicates the resolution of the TFD. A TFD that is highly concentrated around the IF of different signal components will result in a high value of R_t. This measure is defined similarly to R_{id} except that the TFD under comparison is truncated,

$$\rho_t(t,f) = \begin{cases} 1 & \text{when } \rho(t,f) > t_h \max(\rho(t,f)) \\ 0 & \text{otherwise} \end{cases} \tag{14}$$

where $\rho(t,f)$ is the TFD under comparison and t_h is a user defined threshold (selected arbitrarily as 0.75). It must be noted that the response of R_t with respect to this threshold is monotonic and, as

such, will consistently affect the results.

The effect of different operators in forming the EMD–TFD is given in Table I. The operators tested

where the arithmetic mean, a logical OR, and the geometric mean.

TFD	R_{id}	R_t	R
arithmetic	0.38	0.44	0.82
geometric	0.38	0.44	0.82
OR	0.32	0.47	0.79

The response of the measures of interference and energy concentration are given in Table II. The

TFDs that required the definition of particular parameters had these parameters optimally selected

to maximise the performance measures. The parameters optimised were, the energy threshold in the

EMD–TFD (e_t), the window length in the spectrogram (W_l) assuming a Hanning window, the β

parameter in the modified–B distribution, the σ parameter for the Choi–Williams distribution, and

the α or volume parameter for the RGK. The optimisation procedure used a fixed grid, maximisation

procedure where the cost function to be maximised was the addition of the two performance measures,

$R = R_{\mathrm{id}} + R_t$. The optimal parameter chosen of each TFD is shown in last column of Table II.

Similar analysis was performed in the presence of 100 realisations of additive white Gaussian noise.

The outcome of these results is shown in Table III, where $R_x = R_{\mathrm{id}} + R_t$, the subscript, x, denotes

the signal to noise ratio (SNR) in decibels and the results are presented as mean (standard deviation)

over 100 realisations. The TFDs were implemented with the optimal parameters shown in Table II.

B. Component estimation

The ability of the EMD–TFD to estimate the IF of a signal component was tested using an automated

method for extracting the IF of a signal component from a TFD. The IF estimator proposed in [18] is

used. This IF estimation procedure uses image processing techniques, namely edge linking algorithms,

TABLE II

TIME–FREQUENCY PERFORMANCE OF VARIOUS TFDs

TFD	R_{id}	R_t	R	optimal parameter value
WVD–EMD	0.28	0.37	0.65	–
EMD–TFD	0.38	0.44	0.82	$e_t = 0.54$
WVD	0.18	0.27	0.45	–
spectrogram	0.25	0.33	0.58	$W_l = 137$
modified–B	0.30	0.40	0.70	$\beta = 0.23$
Choi–Williams	0.28	0.36	0.64	$\sigma = 67$
RGK	0.34	0.41	0.75	$\alpha = 3.69$
HHT	0.11	0.21	0.32	–

TABLE III

NOISE PERFORMANCE OF VARIOUS TFDs

TFD	R_∞	R_{20}	R_{10}	R_3	R_0
WVD–EMD	0.65	0.63 (0.03)	0.53 (0.03)	0.35 (0.04)	0.22 (0.05)
EMD–TFD	0.82	0.78 (0.01)	0.71 (0.02)	0.54 (0.04)	0.40 (0.05)
WVD	0.45	0.43 (0.01)	0.35 (0.03)	0.22 (0.04)	0.15 (0.05)
spectrogram	0.58	0.53 (0.03)	0.47 (0.04)	0.40 (0.04)	0.36 (0.04)
modified–B	0.70	0.70 (0.01)	0.63 (0.02)	0.46 (0.03)	0.33 (0.04)
Choi–Williams	0.64	0.62 (0.01)	0.53 (0.03)	0.38 (0.03)	0.28 (0.03)
RGK	0.75	0.75 (0.01)	0.74 (0.03)	0.72 (0.02)	0.67 (0.03)
HHT	0.32	0.42 (0.03)	0.25 (0.03)	0.15 (0.03)	0.10 (0.03)

to detect signal components.

The results of the IF estimation procedure on each component of a two component signal ($s(t) = s_1(t) + s_3(t)$) based on the selected TFDs are shown in Fig. 5. A two component signal was tested as the automated method of IF extraction mentioned above has difficulty separating components that share similar regions of the time–frequency domain, as seen at the intersection between $s_1(t)$ and $s_2(t)$ and to avoid excessive bias towards TFDs that were designed to represent only LFM components such

as the RGK. The variance is estimated using 100 realisations of additive white Gaussian noise and normalised frequency. In the case where more than two components were found, the components that best approximated the LFM and QFM were used to estimate the variances. Note, that the LFM and QFM components could not be located in the HHT across all noise levels and the QFM component could not be located in the RGK across all noise levels.

C. Real Underwater Acoustic Signal

The EMD–TFD was then applied to an underwater acoustic signal. The signal under test is a segment of humpback whale song recorded using a hydrophone. The EMD–TFD is plotted along with the WVD in Fig. 6.

D. Discussion

The multiple view approach was initially designed with several pre–defined filters or views opti- mised to detect linear FM components. The use of a nonstationary signal decomposition results in adaptive filter design that can be more accurately focussed on the regions of high energy in the joint time–frequency domain and requires no *a priori* information. In fact, a composite multiple view TFD can be constructed using any appropriate signal decomposition. The EMD is particularly suited to a multiple view framework as it aims to decompose a signal into a series of monocomponents that can be represented by the model outlined in (1) of which QTFDs are ideally suited to represent. This is reflected in the results which show improved representation of the time–frequency energy compared to nonadaptive TFDs and comparable IF estimation performance to the WVD. In fact, the IF estimation method applied to the EMD–TFD generates less candidate signal components compared to the WVD (a reduction of 17% averaged across noise levels) which means that any post–hoc analysis to determine whether the detected component is associated with a real signal component should be simplified.

The disadvantage of the EMD–TFD is that it is computationally more expensive than other methods due to the addition of an EMD algorithm and the calculation of a number of ambiguity domain

representations. The other disadvantage of the EMD–TFD is that when the EMD fails to accurately deompose a signal the EMD–TFD default to a smoothed TFD, such as the Choi–Williams distribution, which can be more efficiently implemented.

The applicability of the EMD–TFD is limited by the performance of the EMD which is known to approximate a filter bank with dyadic cutoff frequencies, much like a wavelet decomposition, in the presence of significant noise [15]. A composite QTFD estimated directly from the IMFs, such as the EMD–WVD, will, as a result, have little relationship to the actual time–frequency behaviour of the signal. The use of ambiguity domain filtering rather than the direct mapping of the IMFs using a QTFD is more robust with, and without the presence of additive white noise. This means that signals that are not accurately decomposed by the EMD will still be represented by a smoothed WVD. This is shown in the Fig. 6 where the interference reduction is generated primarily by the smoothing filter, $h(\nu, \tau)$, rather than the characteristics of the IMFs. It is also shown by the higher correlation measures for the EMD–TFD compared to the WVD–EMD. The EMD–TFD also provides a more accurate representation of signal energy in the joint time–frequency domain compared to the HHT which has the poorest performance of the analysed TFDs.

The EMD algorithm forces continuity of time on each IMF. This means that unrelated signal components are grouped together if they occur at separate times in the signal. A recently proposed modification to the EMD algorithms using the DCT to remove the restriction of continuity in time on an IMF should provide additional improvement in the EMD–TFD [14]. This may help remove interference by components that are separated in time, rather than frequency (the effects of such interference can be seen in Fig. 6(a) at [128ms, 2.5kHz] and [192ms, 3kHz]). Furthermore, additional improvements in the EMD algorithm for decomposing nonstationary multicomponent signals will directly improve the performance of the EMD–TFD as more accurate localisation of the ambiguity domain signal energy can, potentially, be achieved.

The technique used to adapt the filter or view according to energy localisation about the origin is similar to that used in the RGK. The assumption that there is no cross term energy in the ambiguity

domain, due to the signal under analysis being mono–component, means that the proposed method is more suitable for signals that have nonlinear IF laws. This is unlike the RGK which is optimised for only linear FM signals. This explains why the RGK has improved performance in the presence of noise as its ability to resolve the LFM components outweighs its inability to resolve the QFM component. It also explains why the IF estimation procedure cannot extract the QFM signal component from the TFD generated by the RGK.

The EMD–TFD, like many adaptive TFDs, does not satisfy mathematically desirable properties of a QTFD such as marginals, non–negativity, finite support, [3, pp. 60–62]. It does, however, satisfy more general characteristics of a TFD such as real valuedness and energy concentration around the IF law of a signal component [3, pp. 11–12]. These characteristics are important for real world applications such as signal component detection and estimation. Marginals can be enforced by setting the axes of the ambiguity domain to one [11].

It must also be noted, that other high resolution TFDs can be formed using techniques such as short–time kernel adaption, the S–method, and reassignment but these are different in concept and implementation compared to ambiguity domain filtering, [3]. The advantage of using the EMD is that optimisation processes such as these may be more successfully implemented on each IMF than on the original signal. For example, when using the adaptive spectrogram the estimation of the optimal window length may be performed on each IMF and a composite, multiple view spectrogram constructed.

IV. CONCLUSION

This paper proposes a composite TFD based on a multiple view approach. The IMFs of an EMD are used to construct a series of views in the ambiguity domain by highlighting concentrations of energy in the ambiguity domain. The advantage of such a method is that it can overcome interference in TFDs generated by the existence of multiple signal components at the cost of increased computation. The EMD–TFD has been shown to offer superior performance when representing time–frequency energy concentration, and estimating the IF, of nonstationary signal components. The quality of the

signal decomposition technique, however, is critical and it must decompose the signal according to a

well known nonstationary multiple component signal model and be robust in the presence of noise.

REFERENCES

[1] Stevenson, N., Mesbah, M., and Boashash B.: 'A time–frequency distribution based on the empirical mode decomposition'. Proceedings of the International Symposium on Signal Processing Applications, February 2007, Sharjah, UAE, pp. 485–488

[2] Gaunaurd, G.C., and Strifors H.C.: 'Signal analysis by means of time–frequency (Wigner–type) distributions–Applications to sonar and radar echoes', Proceedings of the IEEE, 1996, 84, (9), pp. 1231–1248

[3] Boashash, B., (Ed.), 'Time frequency signal analysis and processing: A comprehensive reference': (Elsevier, 2003, 1st edn.)

[4] Boashash, B., and O'Shea, P.: 'A methodology for detection and classification of some underwater acoustic signals using time–frequency analysis tecnhiques', IEEE Transactions on Acoustics, Speech and Signal Processing, 1990, 38, (11), pp. 1829–1841

[5] Boashash, B., 'Time–frequency signal analysis', in Haykin, S. (Ed.): 'Advances in Spectrum Analysis and Array Processing' (Prentice Hall, 1991, 1st edn.), pp. 418–517

[6] Bedrosian, E.: 'A product theorem for Hilbert transforms', Proceedings of the IEEE, 1963, 51, pp. 686–689

[7] Mallat, S.,: 'A Wavelet Tour of Signal Processing', (Academic Press, 1999, 2nd edn.)

[8] Mallat, S., and Zhang, Z.: 'Matching pursuits with time–frequency dictionaries', IEEE Transactions on Signal Processing, 1993, 41, (12), pp. 3397–3415

[9] Huang, N.E., Shen, Z., Long, S.R., Wu, M.C., Shih, H.H., Zheng, Q., Yen, N.-C. Yen, Tung, C.C., and Liu, H. : 'The empirical mode decomposition and the Hilbert spectrum for nonlinear and non–stationary time series analysis', Proceedings of the Royal Society: Series A, 1998, 454, pp. 903–995

[10] Choi, H.I., and Williams, W.J.: 'Improved time–frequency representation of multicomponent signals using exponential kernels', IEEE Transactions on Acoustics, Speech & Signal Processing, 1989, 37, (6), pp. 862–871

[11] Jones, D.L., and Baraniuk, R.G.: 'A simple scheme for adapting time–frequency representations', IEEE Transactions on Signal Processing, 1994, 42, (12), pp. 3530–3535

[12] Frazer, G., and Boashash, B.: 'Multiple view time–frequency distributions', Proceedings of the Asilomar Conference on Signals, Systems and Computers, Pacific Grove, USA, November 1993, pp. 513–517

[13] Frazer, G.J.: 'Aspects of time-varying non–Gaussian non–linear signal analysis', PhD Thesis., Queensland University of Technology, 1996

[14] Stevenson. N., Mesbah, M., Boashash, B., and Whitehouse, H.J.: 'A joint time–frequency empirical mode decomposition for nonstationary signal separation'. Proceedings of the International Symposium on Signal Processing Applications, February 2007, Sharjah, UAE, pp. 282–285

[15] Flandrin P., Rilling, G., and Goncalves, P.: 'Empirical mode decomposition as a filter bank', IEEE Signal Processing Letters, 2004, 11, (2), pp. 112–114

[16] Huang, N.E., Shen, Z., and Long, S.R.: 'A new view of nonlinear water waves: The Hilbert spectrum', Annual Review of Fluid Mechanics, 1999, 31, pp. 417–457

[17] Rankine, L., Stevenson, N., Mesbah, M., and Boashash, B.: 'A quantitative comparison of non–parametric time–frequency representations'. Proceedings of European Conference on Signal Processing, September 2005, Antalya, Turkey, CD–ROM

[18] Rankine, L., Mesbah, M., and Boashash, B.: 'IF estimation for multicomponent signals using image processing techniques in the time–frequency domain', Signal Processing, 2007, 87, (6), pp. 1234–1250

1) Figure 1: The multiple view composite TFD.

2) Figure 2: The ideal TFD of the synthetic test signal.

3) Figure 3: The ambiguity domain filter set or views for the EMD–TFD.

4) Figure 4: Several TFDs of the simulated multiple component signal. The contours are set to 65% of the maximum value of the quadratic FM component.

5) Figure 5: The variance of the IF estimates using edge–linking on a TFD.

6) Figure 6: The EMD–TFD and WVD of a segment of whale song (A 2D Hanning filter is used and $e_t = 0.05$).

(a) general
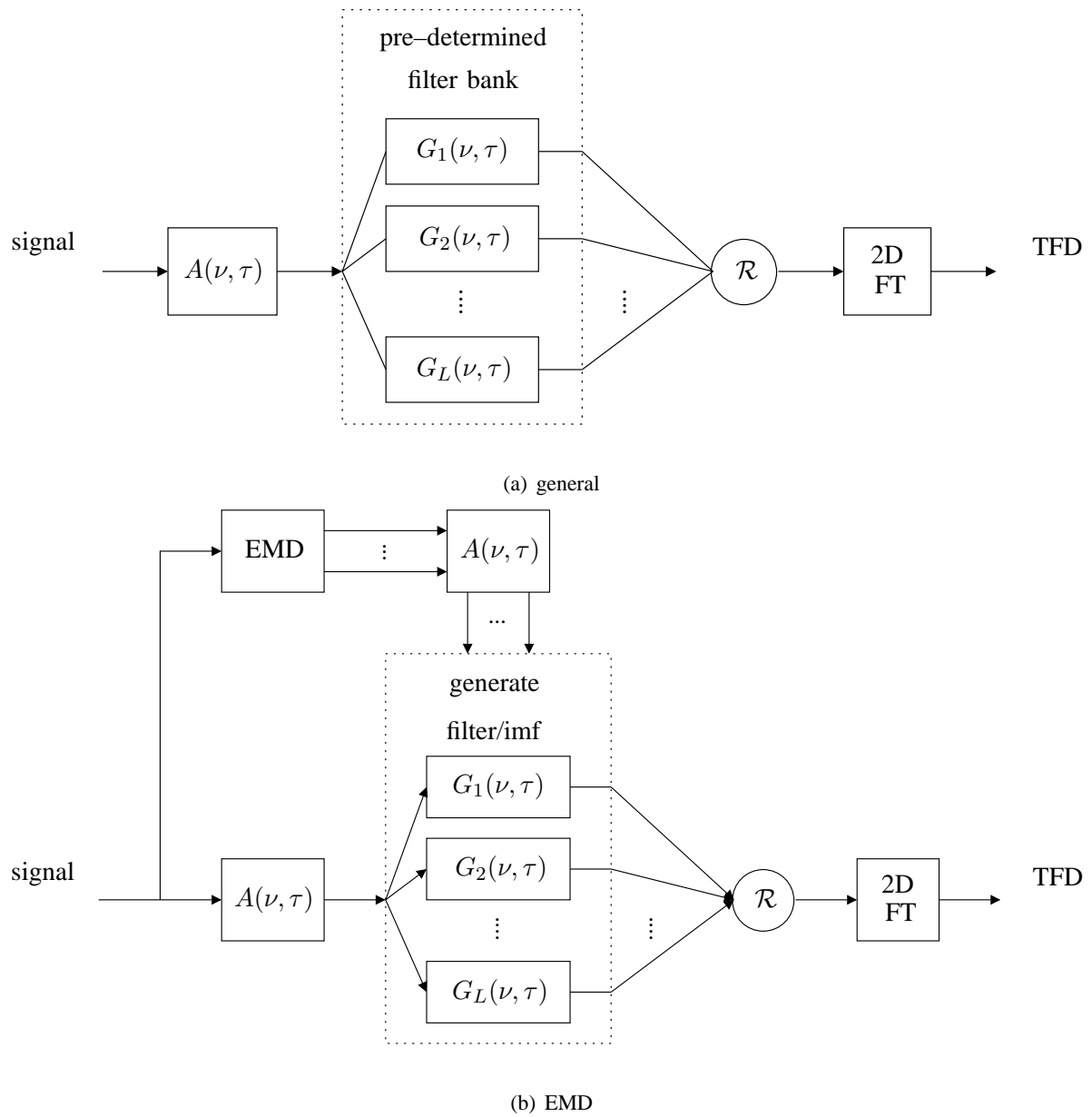
(b) EMD

Fig. 1.   The multiple view composite TFD.
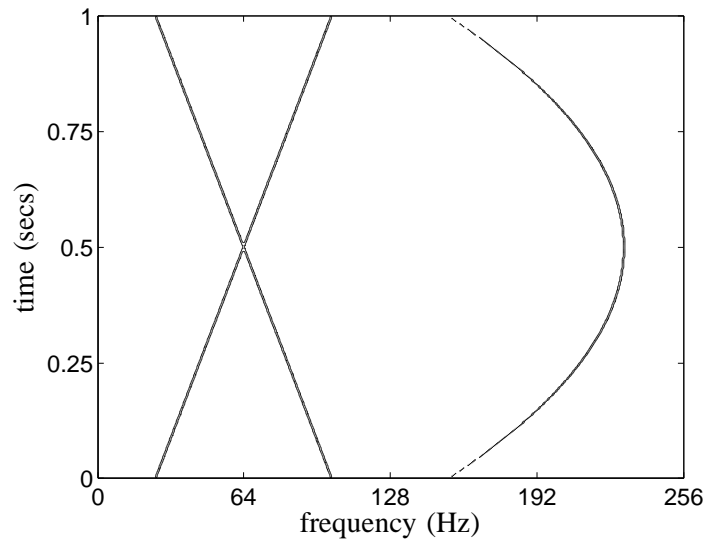
Fig. 2.   The ideal TFD of the synthetic test signal.
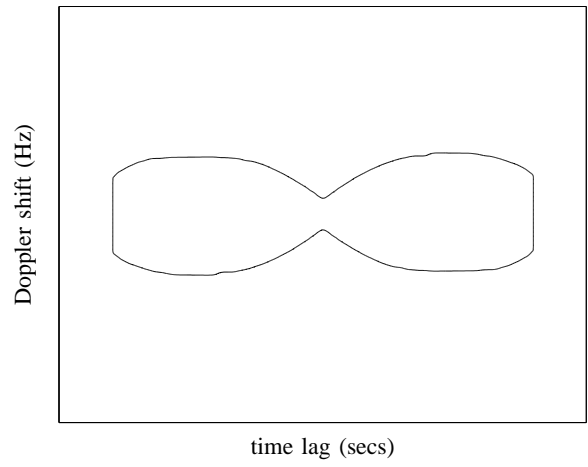
(a) $G_1(\nu, \tau)$
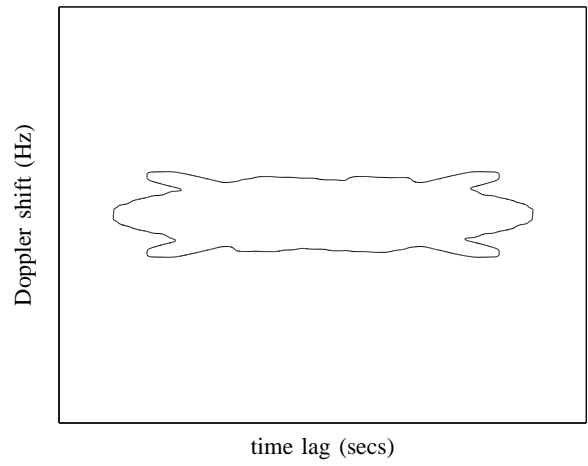
(b) $G_2(\nu, \tau)$
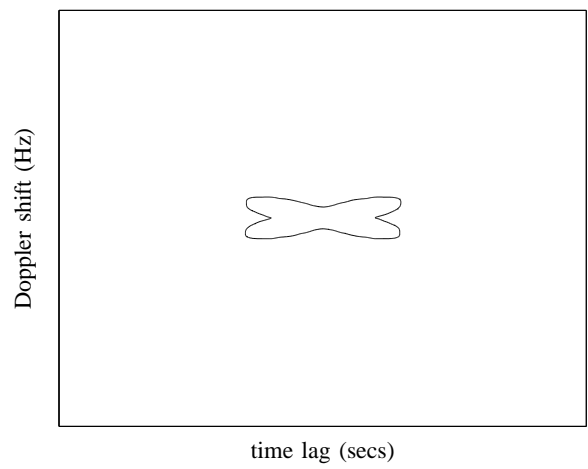
(c) $G_3(\nu, \tau)$

Fig. 3.   The ambiguity domain filter set or views for the EMD–TFD.
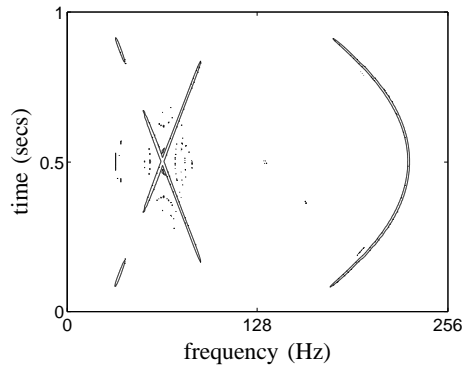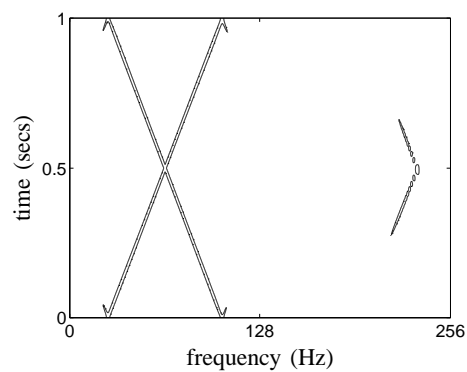
(a) WVD–EMD
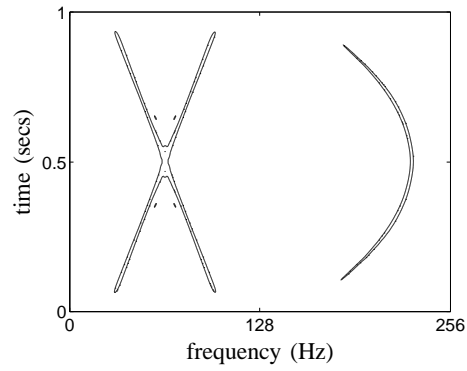
(b) EMD–TFD
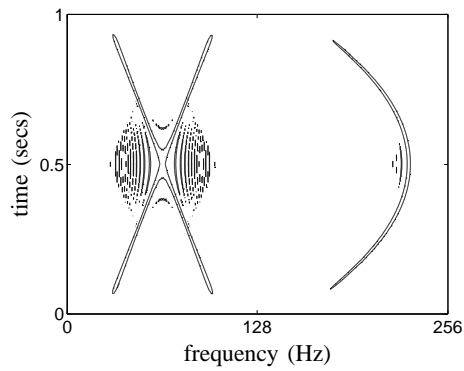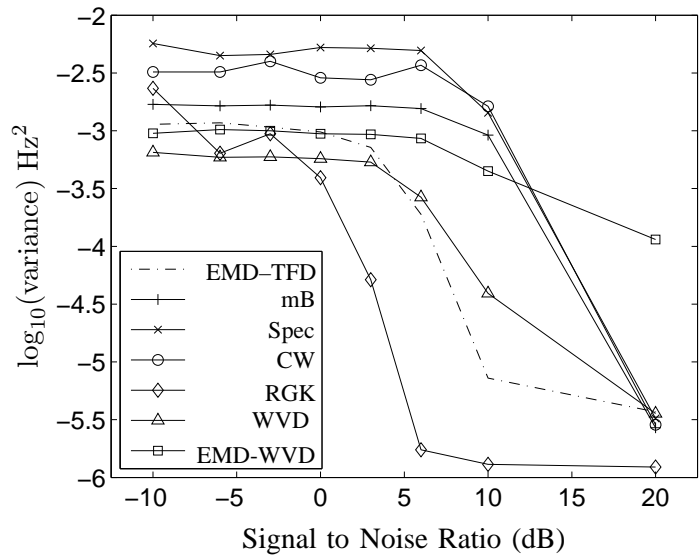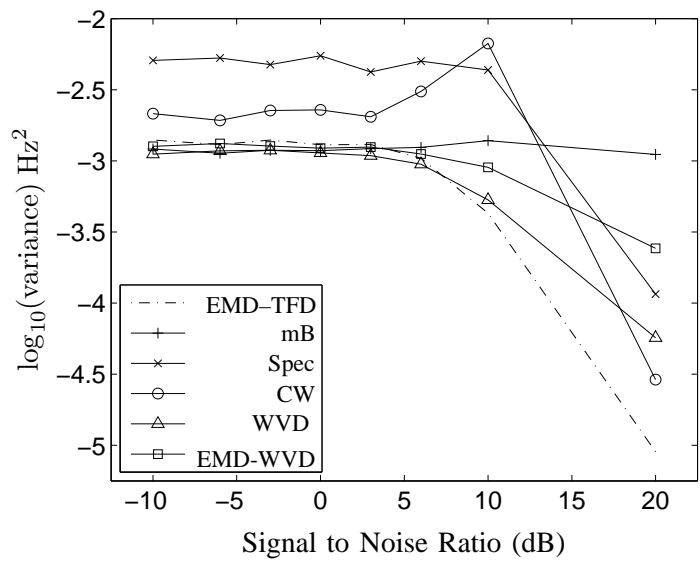
(c) modified B
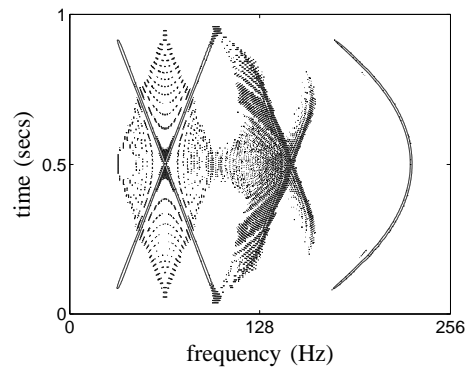
(d) WVD
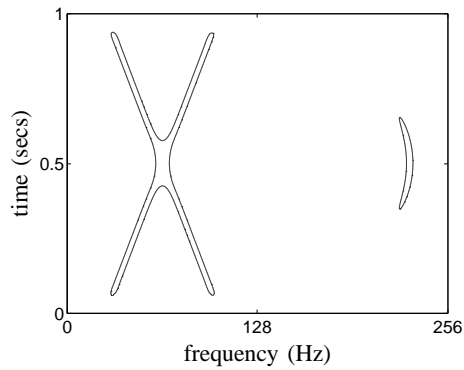
(e) Spectrogram
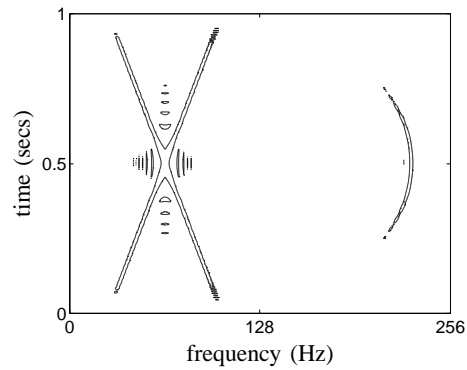
(f) Choi–Williams
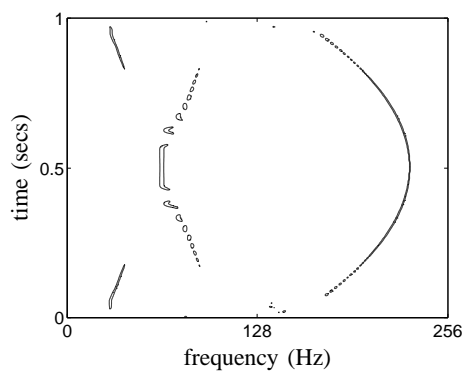
(g) HHT

(h) RGK

Fig. 4.   Several TFDs of the simulated multiple component signal. The contours are set to 65% of the maximum value of the quadratic FM component.
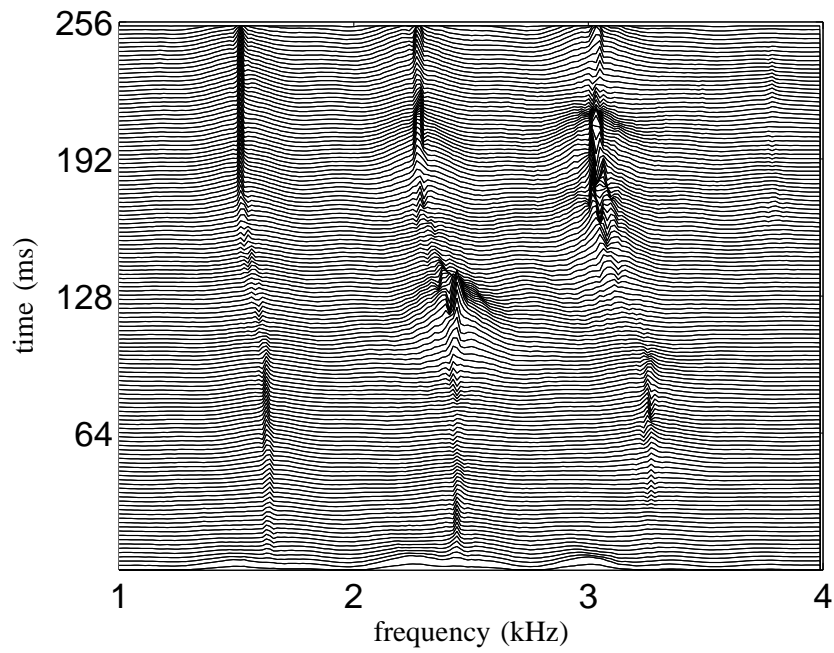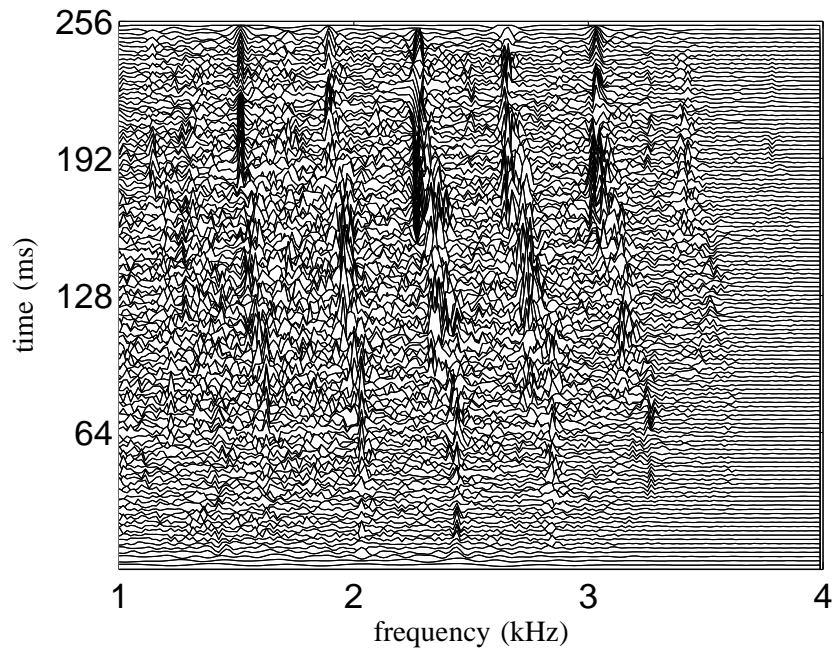
(a) LFM component

(b) QFM component

Fig. 5.   The variance of the IF estimates using edge–linking on a TFD.

(a) EMD–TFD

(b) WVD

Fig. 6.   The EMD–TFD and WVD of a segment of whale song (a 2D Hanning filter is used and $e_t = 0.05$).